Depósito de investigación de la Universidad de Sevilla

https://idus.us.es/

"This document is the Accepted Manuscript version of a Published Work that appeared in final form in Journal of Agricultural and Food Chemistry, copyright © American Chemical Society after peer review and technical editing by the publisher. To access the final edited and published work see https://doi.org/10.1021/acs.jafc.9b07147."

Neuroprotective and anti-inflammatory effects of pterostilbene metabolites in human neuroblastoma SH-SY5Y and RAW 264.7 macrophage cells

Pablo Peñalver,[†,*] Sonia Zodio,[†] Ricardo Lucas,[‡] María Violante de-Paz[‡] and Juan Carlos Morales[†,*]

Affiliations

[†]Department of Biochemistry and Molecular Pharmacology, Instituto de Parasitología y Biomedicina López Neyra, CSIC, PTS Granada, Avda. del Conocimiento, 17, 18016 Armilla, Granada, Spain.

[‡]Department of Organic and Pharmaceutical Chemistry, School of Pharmacy, University of Seville, c/ Prof. García González, 2, 41012, Seville, Spain.

KEYWORDS

Polyphenols, neuroprotective effect, inflammation, metabolites.

ABSTRACT

Oxidative stress is known to be a key factor in many neurodegenerative diseases. Inflammation also plays a relevant role in a myriad of pathologies such as diabetes and atherosclerosis. Polyphenols coming from dietary sources, such as pterostilbene, may be beneficial in this type of diseases. However, most of them are rapidly metabolized and excreted yielding very low phenolic bioavailability what makes difficult to find out which are the mechanisms responsible for the observed bioactivity. Herein, we evaluate the effects of pterostilbene and its metabolites against H_2O_2-induced cell damage in human neuroblastoma SH-SY5Y cells and against LPS-challenged RAW 264.7 macrophages. Among the metabolites tested, 3-methyl-4´-glucuronate-resveratrol (also called 4'-glucuronate pinostilbene, PIN-GlcAc, **11**) prevented neuronal death via attenuation of ROS levels and increased REDOX activity in neurons. This compound is also able to ameliorate LPS-mediated inflammation on macrophages via inhibition of IL-6 and NO production. Thus, polyphenol from dietary sources could be part of potential functional foods designed to ameliorate the onset and progression of certain neurodegenerative diseases *via* oxidative stress reduction.

INTRODUCTION

Oxidative stress is known to be a relevant factor in the progress of neurodegenerative diseases such as Alzheimer's disease, Parkinson's disease or ischemia.[1] Stress is caused by a disparity between the reactive oxygen species (ROS) and reactive nitrogen species (RNS) generated, and the endogenous antioxidants present in cells.[2] ROS are usually detected in apoptotic cell death as well as in neurodegenerative processes in the brain.[3]

Inflammation is the defense mechanism of the human body to injurious stimuli, such as tissue harm, trauma, or infection. It is mediated by activated immune cells such as monocytes and macrophages.[4] Chronic inflammation is related to a wide variety of diseases such as asthma, psoriasis, obesity, atherosclerosis or cancer.[5] Thus, clinical strategies to fight chronic inflammation and related diseases like cancer include blocking theinflammatory responses and the inhibition of proinflammatory mediator production.

Inflammation is mediated by inflammatory cytokines such as interleukins IL-6 and IL-1β, tumor necrosis factor (TNF)-α, interferon (IFN)-γ and by inflammatory mediators, such as nitric oxide (NO) and prostaglandin E2 (PGE2).[6] The main pro-inflammatory stimuli comprise cytokines, UV irradiation, mitogens and bacterial lipopolysaccharide (LPS) which modulate their effects by inducing the activation of transcription factor NFκB.[7-8]

Dietary polyphenols have been reported to display anti-apoptotic, anti-inflammatory and antioxidant properties (preventing proteins oxidation, lipid peroxidation, and ROS generation, having thus a potential neuroprotective effect). In fact, these effects have been observed on *in vitro* and *in vivo* models of toxicity and neurological disorders.[9-10] Moreover, polyphenols from red wine, nuts berries and other fruits, such as resveratrol (RES), pterostilbene (PTER) and ellagitannins (ETs), have proven to exert neuroprotective effects on various animal models of neurodegeneration.[11-14] Nonetheless, dietary source polyphenols show poor bioavailability due to an extensive metabolism by colonic microbiota and through phase II metabolism in the liver,[15] preventing them from reaching systemic tissues.[9, 16]

Therefore, the compounds really responsible for the *in vivo* neuroprotective and antioxidant effects of polyphenols are not entirely known. While dietary polyphenols show poor bioavailability, their metabolites can actually reach the brain,[17-22] and the human bloodstream.[23-24] So, phenolic metabolites should be taken into account as potential candidates to exert the biological activity attributed to the polyphenolic dietary precursors. In fact, protocatechuic Acid, a major metabolite of anthocyanins found in green tea, wine and berries, has been reported to prevent PC12 neuronal cells death caused by amyloid-β toxicity.[25] Similarly, González-Sarrías *et al*. showed neuroprotective activity of physiologically relevant polyphenol-derived metabolites such as gallic acid, ellagic acid (EA), 3,4-dihydroxyphenylpropionic acid and 3,4-dihydroxyphenylacetic acid in a H_2O_2-challenged SH-SY5Y cells model.[26]

Pterostilbene (PTER) is a naturally occurring stilbenoid, analogue of RES, mainly found in blueberries. PTER has shown improved oral bioavailability and potency in comparison with RES.[27-28] The antioxidant, anti-inflammatory, and anticancer activity of PTER has been deeply studied in the literature.[29-33] The metabolic fate of PTER in mice was investigated by Shon *et al.*[34] and seven metabolites were detected in urine using liquid chromatography/atmospheric pressure chemical ionization and electrospray ionization tandem mass spectrometry. Two of those metabolites come from direct chemical modification of PTER, its 4'-glucuronate (PTER-GlcAc, **7**) and its 4'-sulphate (PTER-S, **8**) derivatives (see Table 1). The other five metabolites come from modification of two intermediates formed *in vivo* but not detected, the mono-demethylated pterostilbene (also called pinostilbene, PIN, **9**) and the mono-3'-hydroxylated pterostilbene (3'-OH-PTER). These metabolites are PIN-4'-glucuronate (PIN-GlcAc, **11**) and PIN-4'-sulphate (PIN-S, **12**) from PIN (Table 1), and 4'-sulphate-3'-OH-PTER, 4'-glucuronate-3'-OH-PTER and 4'-glucuronate-3'-sulphate-PTER from the intermediate 3'-OH-PTER (not shown in Table 1).
PIN is also found in the amazonian climber *Gnetum venosum* and in the bark of *Pinus sibirica*.[35-36] Most importantly, PIN is a major metabolite of PTER in the colon of mice fed with PTER and another stilbenoid, analogue of RES. PIN has shown to play an important role in the anti-colon cancer effects elicited when PTER was orally administered to mice.[37]

PTER metabolites are probably produced in a similar way to those of RES which is mainly metabolized in the liver into the corresponding mono-glucuronides or mono-sulfates by phase II enzymes and, to a lower extent, into piceatannol by phase I enzymes, and into dihydroresveratrol by human microbiota.[38]

In this paper, the anti-inflammatory and antioxidant activity of several PTER metabolites (compounds **7**-**12**, Table 1), at physiologically relevant concentrations, were determined. RES and its metabolites (compounds **2**-**5**, Table 1) were also prepared and evaluated for direct comparison with the PTER metabolites. An LPS-induced inflammation in RAW 264.7 macrophages and an H_2O_2-induced neurotoxicity in human neuroblastoma SH-SY5Y cells models were chosen for these purposes.

MATERIALS AND METHODS

General information

All chemicals were obtained from chemical suppliers and used without further purification, unless otherwise noted. RES (**1**) and PTER (**6**) were obtained from Sigma Aldrich. All reactions were monitored by TLC on precoated Silica-Gel 60 plates F254, and detected by heating with Mostain (500 ml of 10% H_2SO_4, 25g of $(NH_4)_6Mo_7O_{24}$•$4H_2O$, 1g $Ce(SO_4)_2$•$4H_2O$). Products were purified by flash chromatography with silica gel60 (200-400 mesh). NMR spectra were recorded on 300, 400 or 500 MHz NMR equipment, at room temperature for solutions in $CDCl_3$, D_2O or CD_3OD. Chemical shifts are referred to the solvent signal and are expressed in ppm. 2D NMR experiments (COSY, TOCSY, ROESY, and HMQC) were carried out when necessary to assign the corresponding signals of the new compounds. Sephadex LH 20, Reverse phase column and then ion-exchanged with Dowex 50W were used in the purification of several glucuronic and sulfate metabolites. High resolution mass spectra (HRMS) were obtained on an ESI/quadrupole mass spectrometer (WATERS, ACQUITY H CLASS). If necessary, the purity was determined by high performance liquid chromatography (HPLC). Purity of all final compounds was 95% or higher.

Synthesis

4′-O-(2,3,4-tri-O-pivaloyl-β-D-glucuronic acid methyl ester)-3,5-dimethoxy-Resveratrol (**14**). To a solution of trichloroacetimidate **13**[39] (354 mg, 0.58 mmol) and Pterostilbene **6** (100 mg, 0.39 mmol) in anhydrous CH_2Cl_2 (5 mL) at 0ºC, $BF_3{\cdot}OEt_2$ (0.145 mmol, 18 μL) was added. After 30 min the reaction was warmed at room temperature for another 30 min. TLC showed the formation of a major product and consumption of the glycosyl donor. The reaction was then quenched with NEt_3 and concentrated *in vacuo*. The resulting residue was purified by flash column chromatography (hexane: ethyl acetate from 6:1 to 2:1) to afford **14** (162 mg, 60%) as a yellow glassy solid; δ_H (300 MHz, $CDCl_3$) 7.35 (d, J = 8.7 Hz, 2 H, Harom), 6.97-6.81 (m, 4 H, 2 Harom, 2x=CH), 6.56 (d, J = 2.1 Hz, 2 H, Harom), 6.31 (t, J = 2.1 Hz, 1 H, Harom), 5.42-5.25 (m, 3 H, H-3, H-4, H-2), 5.06 (d, J = 7.5 Hz, 1 H, H-1), 4.16 (d, J = 9.6 Hz, 1 H, H-5), 3.74 (s, 6 H, OCH_3), 3.66 (3 H, $COOCH_3$), 1.08, 1.07 (2 s, 27 H, $C(CH_3)_3$); δ_C (75 MHz, $CDCl_3$) 177.0, 176.5, 176.4, 166.9 (C=O), 160.9, 156.5, 139.3, 132.6, 128.2, 127.9, 127.8, 117.1, 104.5, 99.9 (=C, Carom), 99.5 (C-1), 73.0 (C-5), 71.4 (C-3), 70.5 (C-2), 69.1 (C-4), 55.4, 52.3 (CH_3O), 38.8 ($C(CH_3)_3$), 27.2, 27.1 ($C(CH_3)_3$); (HRMS (ES^+) Calcd. for $C_{38}H_{50}O_{12}Na$ (M^+) 721.3200, found: 721.3186.

Potassium 4′-O-(β-D- glucopyranosyluronic acid)-3,5-dimethoxy-resveratrol (**7**). A suspension of **14** (90 mg, 0.128 mmol) and K_2CO_3 (110 mg, 0.79 mmol) was prepared in a mixture of methanol:water:dioxane (1:1:1, 9 mL), and the mixture was stirred at room temperature for 24 h. Then, KOH (100 mg, 1.78 mmol) was added and the reaction was stirred for 48 h and and later neutralized with IR-120 H^+ resin. The solvents were then removed and the residue was purified by RP-C18 column eluting with water:methanol (1:6) to obtain 40 mg (70 % yield). δ_H (300 MHz, CD_3OD) 7.48 (d, J = 8.7 Hz, 2 H, Harom), 7.14-7.08 (m, 3 H, 2 Harom, 1x=CH), 6.97 (d, J = 16.4 Hz, 2 H, =CH), 6.69 (d, J = 2.1 Hz, 2 H, Harom), 6,38 (t, J = 2.1 Hz, 1 H, Harom), 4.97-4.95 (m, 1 H, H-1), 3.78 (m, 7 H, H-5, OCH_3), 3.55-3.53 (m, 3 H, H-3, H-4, H-2); δ_C (75 MHz, CD_3OD) 174.8 (C=O), 161.0, 157.5, 139.7, 131.7, 128.1, 127.3, 126.9, 116.7, 103.9, 100.1 (=C, Carom), 99.3 (C-1), 76.4 (C-5), 75.2 (C-3), 73.3 (C-2), 72.2 (C-4), 54.4 (CH_3O); (HRMS (ES^+) Calcd. for $C_{22}H_{25}O_9Na$ (M^+) 433.1499, found: 433.1487.

Sodium Resveratrol-3,5-dimethoxy-4'-sulfate (**8**). Pterostilbene (3,5-dimethoxy resveratrol, **6**, 100 mg, 0.39 mmol) was dissolved in dry DMF in a 2-5 mL microwave reaction vial containing magnetic stirrer bar and fitted with a septum, which was then pierced with a needle. Sulfur trioxide–trimethylamine complex (2 eq., 0.78 mmol, 108 mg) was then added (this complex has been previously washed with H_2O, MeOH, and CH_2Cl_2 and dried under high vacuum). Microwave based sulfation reaction was performed using a Biotage Initiator synthesizer in sealed reaction vessels.[40-42] The closed vial was then evacuated under high vacuum for 30 min and the mixture was subjected to microwave radiation for 40 min at 120 ºC (50-60W average power). MeOH (1 mL) and CH_2Cl_2 (1 mL) were added, and the solution was layered on the top of a Sephadex LH-20 chromatography column which was eluted with MeOH to obtain the corresponding triethylammonium salt that was then purified through RP C18 chromatography with MeOH-H_2O (80:20). Finally, the product was eluted through an ion exchange colum with dowex Na^+ to afford the corresponding sodium salt **8** (120 mg, 86% yield). δ_H (300 MHz, CD_3OD) 7.39-7.36 (m, 3 H, Harom), 7.07-6.85 (m, 5 H, 2 Harom, 2x=CH), 6.35 (s, 1 H, Harom),3.78 (s, 6 H, OCH3); δ_C (75 MHz, CD_3OD) 161.0, 160.9, 139.8, 128.9, 128.6, 127.6, 125.3, 115.1 (=C, Carom), 55.4 (CH_3O); (HRMS (ES+) Calcd. for $C_{16}H_{15}O_6S$ (M+) 335.0595, found:.335.0612

(E)-4-[3-Methoxy-5-(tert-butyldimethylsilyloxy) styryl]phenol or 3-Methoxy-5-(tert-butyldimethylsilyloxy)-resveratrol (**15**). To a solution of 3-methoxy-resveratrol (650 mg, 2.68 mmol) in DMF (anhydrous, 10 mL) cooled in an ice-water bath under argon, TBDMSCl (202 mg, 1.34 mmol, 0.5 equiv) and imidazole (225 mg, 3.35 mmol, 1.0 equiv) were added sequentially. The reaction mixture was stirred for 30 min at 0º C and another 30 min at room temperature. The pale yellow reaction mixture was diluted with EtOAc (50 mL), cast into a separatory funnel, and washed with water (2x25 mL), brine (25 mL), and the organic phase was dried (Na_2SO_4). Filtration and concentration in vacuo afforded the crude that was purified by flash column chromatography (hexane:ethyl acetate:methanol from 10:1 to 3:1) to afford **15** (200 mg, 21%). δ_H (300 MHz, $CDCl_3$) 7.45 (d, J = 8.7 Hz, 2 H, Harom), 6.96-6.82 (m, 4 H, 2 Harom, 2x=CH), 6.61 (d, J = 2.0Hz, 2 H, Harom), 6,31 (t, J = 2.0 Hz, 1 H, Harom), 3.85 (s, 3 H, OCH_3), 1.03 (s, 9

H, $C(CH_3)_3$), 0.26 (s, 6 H, $Si(CH_3)_2$); δ_C (75 MHz, $CDCl_3$) 159.3, 157.0, 156.7, 139.8, 130.0, 128.7, 127.8, 126.3, 114.2, 111.0, 106.6, 106.4 (=C, Carom), 55.4 (CH_3O), 25.7 ($C(CH_3)_3$), 18.2 ($C(CH_3)_3$), -4.35 ($Si(CH_3)_2$). (HRMS (ES^+) Calcd. for $C_{21}H_{29}O_3Si$ (M+1) 357.1886, found: 357.1878.

4′-O-(2,3,4-tri-O-pivaloyl-β-D-glucuronic acid methyl ester)-3-methoxy-5-(tert-butyldimethylsilyloxy) Resveratrol (**16**). To a solution of trichloroacetimidate **13** (382 mg, 0.63 mmol) and compound **15** (150 mg, 0.42 mmol) in anhydrous CH_2Cl_2 (5 mL) at 0ºC, $BF_3 \cdot OEt_2$ (0.157 mmol, 20 μL) was added. After 30 min the reaction was warmed at room temperature for another 30 min. TLC showed the formation of a major product and consumption of the glycosyl donor. The reaction was then quenched with NEt_3 and concentrated *in vacuo*. The resulting residue was purified by flash column chromatography (hexane: ethyl acetate from 8:1 to 6:1) to afford **16** (200 mg, 60%) as a yellow glassy solid; δ_H (300 MHz, $CDCl_3$) 7.22 (d, J = 8.7 Hz, 2 H, Harom), 6.79-6.59 (m, 4 H, 2 Harom, 2x=CH), 6.53-6.47 (m, 2 H, Harom), 6,17 (t, J = 2.1 Hz, 1 H, Harom), 5.29-5.11 (m, 3 H, H-3, H-4, H-2), 4.92 (d, J = 7.8 Hz, 1 H, H-1), 4.03 (d, J = 9.9 Hz, 1 H, H-5), 3.62 (s, 3 H, OCH_3), 3.55 (3 H, $COOCH_3$), 0.96, 0.95, 0.94 (3 s, 27 H, $C(CH_3)_3$), 0.78 (s, 9 H, $SiC(CH_3)_3$), 0.00 (s, 6 H, $Si(CH_3)_2$); δ_C (75 MHz, $CDCl_3$) 177.0, 176.5, 176.4, 166.8 (C=O), 159.5, 157.9, 156.8, 139.9, 129.7, 129.1, 127.8, 125.9, 114.1, 113.3, 108.1, 107.9 (=C, Carom), 99.6 (C-1), 72.9 (C-5), 71.5 (C-3), 70.5 (C-2), 69.1 (C-4), 55.3, 52.9 (CH_3O), 38.8, 38.7, 30.9 ($C(CH_3)_3$, Si $C(CH_3)_3$), 27.2, 27.1, 25.6 ($C(CH_3)_3$, $SiC(CH_3)_3$,), -4.42 (Si ($CH_3)_2$); (HRMS (ES^+) Calcd. for $C_{43}H_{62}O_{12}NaSi$ (M^+) 821.3908, found 821.3896.

Potassium 4′-O-(β-D- glucopyranosyluronic acid)-3-methoxy-resveratrol (**11**). A suspension of **16** (150 mg, 0.187 mmol) and KF (2eq., 22 mg, 0.374 mmol) was prepared in methanol (4 mL) and stirred for 2 h. Then, K_2CO_3 (180 mg, 1.30 mmol) was added and the mixture was stirred at room temperature for 24 h. Later, KOH (100 mg, 1.78 mmol) was added and reaction was stirred for 48 h, and finally, it was neutralized with IR-120 H^+ resin. The solvents were removed and the residue was purified by RP-C18 column eluting with water:methanol (1:6). Fractions containing the major product were concentrated to afford compound **11** (65 mg, 84%). δ_H (300 MHz,

CD_3OD) 7.22 (d, J = 8.7 Hz, 2 H, Harom), 6.79-6.59 (m, 4 H, 2 Harom, 2x=CH), 6.53-6.47 (m, 2 H, Harom), 6,17 (t, J = 2.1 Hz, 1 H, Harom), 5.29-5.11 (m, 3 H, H-3, H-4, H-2), 4.92 (d, J = 7.8 Hz, 1 H, H-1), 4.03 (d, J = 9.9 Hz, 1 H, H-5), 3.62 (s, 3 H, OCH_3), 3.55 (3 H, $COOCH_3$), 0.96, 0.95, 0.94 (3 s, 27 H, $C(CH_3)_3$), 0.78 (s, 9 H, $SiC(CH_3)_3$), 0.00 (s, 6 H, $Si(CH_3)_2$); δ_C (75 MHz, $CDCl_3$) 177.0, 176.5, 176.4, 166.8 (C=O), 159.5, 157.9, 156.8, 139.9, 129.7, 129.1, 127.8, 125.9, 114.1, 113.3, 108.1, 107.9 (=C, Carom), 99.6 (C-1), 72.9 (C-5), 71.5 (C-3), 70.5 (C-2), 69.1 (C-4), 55.3, 52.9 (CH_3O), 38.8, 38.7, 30.9 ($C(CH_3)_3$, Si $C(CH_3)_3$), 27.2, 27.1, 25.6 ($C(CH_3)_3$, $SiC(CH_3)_3$,), -4.42 (Si ($CH_3)_2$); (HRMS (ES^+) Calcd. for $C_{43}H_{62}O_{12}NaSi$ (M^+) 821.3908, found 821.3896.

3-Methoxy-4'sulfate-resveratrol (**12**). Compound **15** (220 mg, 0.61 mmol) was dissolved in dry acetonitrile in a 2-5 mL microwave reaction vial containing a magnetic stirrer bar and fitted with a septum, which was then pierced with a needle. Sulfur trioxide–trimethylamine complex (2 eq., 1.23 mmol, 170 mg) (this complex has been previously washed with H_2O, MeOH, and CH_2Cl_2 and dried under high vacuum) and NEt_3 (1ml) were then added. Microwave based sulfation reaction was carried out using a Biotage Initiator synthesizer in sealed reaction vessels. The closed vial was evacuated under high vacuum for 30 min and the mixture was subjected to microwave radiation for 30 min at 100 ºC (50-60W average power). Solvents were removed under vacuo and the crude was used for the next step without further purification. Next, the crude (220 mg, 0.44 mmol) and KF (51 mg, 0.88 mmol) were dissolved in MeOH (10 mL). The reaction mixture was stirred at room temperature for 18 h and the solvent was removed under vacuo. The crude was purified by Sephadex LH 20 eluting with MeOH. Fractions containing the desired product were concentrated and dried affording compound **12** (85 mg, 54% yield). δ_H (300 MHz, CD_3OD) 7.45(d, 2 H, Harom), 6.99 (d, 1 H, =CH), 6.92-6.82 (m, 3 H, =CH, Harom), 6.48 (d 2 H, J = 2.1 Hz, Harom), 6.20 (t, 1 H, J = 2.1 Hz, Harom), 3.80 (s, 3 H, OCH_3); δ_C (75 MHz, $CDCl_3$) 159.4, 158.3, 139.9, 130.1, 128.9, 128.3, 127.7, 127.4, 127.3, 126.4, 113.7, 104.5, 99.9, 54.3; (HRMS (ES^+) Calcd. for $C_{15}H_{13}O_6S$ (M^-) 321.048, found: 321.0434.

245 **Biological evaluation**

246 ***Cell cultures.*** SH-S5Y5 neurons were cultured in collagen-pretreated petri-dishes (100ug/ml
247 collagen in 0.02N acetic acid) with DMEM-F12 medium supplemented with
248 Penicillin/Streptomycin and 10 % inactivated fetal bovine serum (iFBS). Cells were split every
249 other day and the cell confluence was maintained above 40% at all time.

250 RAW 264.7 macrophages were cultured in 75cm^2 flasks with DMEM high glucose medium
251 supplemented with Penicillin/Streptomycin and 10 % iFBS. Cells were split every other day. A
252 cell scraper was necessary to detach cells from the flask after trypsinization.

253 ***Cell viability assays.*** Neuron assays were carried out in collagen-pretreated 96 well plates by
254 seeding 2 x 10^4 neurons per well in a 100 μL volume and with 24 h of incubation time before
255 compound addition. Macrophage assays were carried out in 96 well plates by seeding 2.5 x 10^4
256 macrophages per well in a 100 μL volume with 4 h of incubation time before compound addition.
257 10, 1 and 0.1 mM DMSO stocks of the tested compounds were prepared. 1:100 dilutions of each
258 stock in cell culture media were prepared upon addition of the compounds to the well plate. Thus,
259 the final compound concentrations in the plate were 100, 10 and 1 μM respectively, whereas the
260 DMSO percentage in each cell was 1%. The cytotoxic effect was calculated by mitochondrial
261 MTT assay, according to manufacturer 24 hours after compound addition as the percentage of
262 cell proliferation values with respect to the control cells (w/o DMSO; 100%). Data are presented
263 as the mean ± SD of at least eight measurements.

264 ***Neuroprotective assay.*** Neurons were cultured and plated as described in the cell viability
265 assay. Tested compounds dissolved in DMSO (10, 1 and 0.1 mM stocks) were added to the plate
266 at different concentrations (100, 10 and 1 μM, respectively) as in the cell viability assays and the
267 final DMSO percentage in each cell was adjusted to 1%. Right away (co-incubation experiments)
268 or after 6 hours incubation (pre-incubation experiments), 100 μM of hydrogen peroxide (30%
269 w/w in water) was added. Cell viability was evaluated 24 hours after compound addition by
270 mitochondrial MTT assay, according to manufacturer. The percentage of cell proliferation values

271 are referred to the control cells (1% DMSO w/o hydrogen peroxide; 100%). Data are presented
272 as the mean ± SD of at least eight measurements

273 ***Anti-inflammatory analysis*.** RAW 264.7 macrophages were cultured and plated as described
274 in the cell viability assay. Tested compounds dissolved in DMSO were added at different final
275 concentrations (100, 10 and 1 μM) to the well plate and the final DMSO percentage in each cell
276 was adjusted to 1%. Right away (co-incubation experiments) or after 6 hours incubation (pre-
277 incubation experiments), 100 ng /mL of LPS was added. The cytotoxic effect was calculated by
278 mitochondrial MTT assay, according to manufacturer 24 hours after compound addition as the
279 percentage of cell proliferation values with respect to the control cells (1% DMSO w/o LPS;
280 100%). Data are presented as the mean ± SD of at least eight measurements.

281 ***Measurement of Reactive Oxygen Species (ROS)***. The ROS-sensitive 2′,7′-
282 dichlorodihydrofluorescein diacetate (H2DCFDA) staining method (Sigma, St. Louis, MO, USA)
283 was used to perform the ROS measurements, as previously described in the literature.[26] Neurons
284 were seeded and treated as in the cell viability assays. After the treatments, the culture medium
285 was removed and a 25 μM H2DCFDA solution in DMSO (100uL/well) was added to the 96 well
286 plates. Following a 2 h incubation at 37 °C in the dark the fluorescence intensity was measured
287 at an excitation/emission pairs of 495/520 nm in a multimode microplate reader (TECAN Infinite
288 F200, Tecan Trading AG, Switzerland). The relative amount of intracellular ROS were calculated
289 in relation to the untreated control cells (100%). Data are presented as the mean ± SD of at least
290 eight measurements.

291 ***Measurement of Mitochondrial Oxidation−Reduction (REDOX) Activity***. Resazurin (Life
292 Techonologies Inc., Rockville, MD, USA), a fluorogenic oxidation-reduction indicator, was used
293 to perform the analysis of REDOX activity. Neurons were seeded and treated as in the cell
294 bioability assays. Resazurin (5 μM in water) was added to the wells after treatments and the
295 fluorescence intensity was checked 2h later at an excitation/ emission pair of 530/590 nm in the
296 microplate reader described above. The relative amount of REDOX activity was calculated in

relation to the untreated control cells (100%). Data are presented as the mean ± SD of at least eight measurements.

IL-6 inhibition studies. To determine cytokine production, 5×10^5 RAW 264.7 macrophages were seeded in 24-well plates (in 0.5 ml). Compounds (10μM) were then added and macrophages were either stimulated or not by adding LPS (1μg/ml) to the medium. After 24 hr, levels of IL-6 in the supernatants were determined by ELISA using capture/biotinylated detection antibodies from BD PharMingen and PrepoTech.[43-45] The concentration of IL-6 present in the supernatant of treated cells (in ng/ml) is then plotted and compared to that of LPS stimulated cells (1μg/ml LPS). A minimum of two independent sets of experiments and three replicates per experiment were carried out. All data are expressed as mean ± SD.

Determination of NO. Cells were seeded, stimulated with LPS and treated with our compounds in the same way as in the IL-6 inhibition assay. The amount of NO formed was estimated from the accumulation of the stable NO metabolite nitrite by the Griess assay.[42] Equal volumes of culture supernatants (100 μl) and Griess reagents (100 μl of 1% sulfanilamide/0.1% N-[naphthyl]ethyl-enediamine dihydrochloride in milliQ water) were mixed, and the absorbance was measured at 540 nm. The amount of nitrite was estimated from a NaNO2 standard curve. The concentration of NO calculated (in ng/ml) is then compared to that of cells stimulated with 1μg/ml LPS. A minimum of two independent sets of experiments and three replicates per experiment were carried out. All data are expressed as mean ± SD.

***Statistical Analysis*.** Data are described as mean values ± SD. Microsot Excel 2010 was used to plot the experimental data. Two-tailed unpaired Student's t test was chosen for statistical analysis. Samples were considered as heterocedastic (unequal variances), as a result of a previously run F test. A p value <0.05 was considered as statistically significant.

RESULTS AND DISCUSSION

Synthesis of PIN (9). PIN was prepared by random alkylation of RES in DMF using K_2CO_3 and iodomethane.[46-47] Subsequent chromatographic separation afforded the mono-, di- and trimethylated resveratrol derivatives. Whereas PTER (**6**) could not be isolated from the dimethylated isomeric mixture under the chromatographic conditions used, the monomethylated derivatives, pinostilbene (PIN, **9**) and compound **10** were obtained. RES (**1**) and PTER (**6**) were obtained from Sigma Aldrich. Compound characterization was easily carried out using NMR spectroscopy due to the differences in symmetry between the mono-substituted regioisomers and, similarly betweento the dimethylated regioisomers.

Synthesis of RES and PTER sulfate metabolites. RES sulfate metabolites (**2-4**), were prepared according to the synthetic procedure of Hoshino *et al*.[48] and to our improved purification methodology previously reported (Scheme 1).[40] PTER (**8**) and PIN (**12**) sulfate metabolites were synthesized following the same procedure. Briefly, PTER (**6**) or the 3'-TBDMS derivative of PIN (**9**) were dissolved in acetonitrile and treated with $SO_3{\cdot}NMe_3$ and NEt_3 under microwave irradiation. The crude of the PTER reaction was first purified by LH-20 gel filtration chromatography and then by reversed-phase chromatography. In the case of PIN, desilylation with KF in MeOH was carried out after the first purification step and the final crude was purified by reverse-phase chromatography. The yields obtained for PTER sulfate (**8**) and PIN sulfate (**12**) were 86 % and 54 % (from 3-methyl-5-TBS-PIN), respectively.

Synthesis of RES and PTER glucuronate metabolites. PTER (**7**) and PIN (**11**) glucuronate metabolites were prepared using the same methodology reported by our group for the synthesis of RES glucuronate (**5**).[49] Briefly, glucuronate metabolites **7** and **11** were synthesized by chemical glycosylation of PTER (**6**) and 3-TBDMS-protected stilbenoid derivative of PIN (**15**), respectively, using a pivaloyl-protected-glucuronate trichloroacetimidate donor (**13**, see schemes 2 and 3).[39] Compound (**15**) was prepared using standard silylation conditions from PIN. Subsequent deprotection of the pivaloyl protecting groups of intermediate **14** (Scheme 2) was

achieved with K_2CO_3 in MeOH/THF/ H_2O to obtain PTER glucuronate **7** (42% yield overall). In the case of PIN, a two-step deprotection was carried out (Scheme3). First, desilylation with KF in MeOH (if required) and then, deacylation with K_2CO_3 in MeOH/THF/ H_2O were carried out to obtain glucoronate **11** (50 % yield overall).

Neuroprotective effects of RES, PTER, PIN and derived Metabolites on H_2O_2-challenged SH-SY5Y cells. All compounds were dissolved in 1% DMSO. RES and its metabolites (**2-5**) did not show any cytotoxic effects when incubated for 24 h using concentrations from 100 to 1 μM, as cell viability 3 was not significantly affected in comparison to the 1% DMSO control (Figure 1). DMSO itself (1% v/v) decreased SH-SY5Y cell viability around 20% compared with the wild type control (Figure 1).

Both, PTER and its metabolites (**6-12**) showed evidence of certain toxicity to neuronal cellsat 100 μM (Figure 1), but this concentration is supra-physiological and then not as relevant as the data resulting from 1 and 10 μM concentrations. PTER (containing two methoxy groups) was more toxic than the mono methoxy derivatives, PIN (**9**) and compound **10**. We could also observe that the glucuronated metabolites of PTER and PIN (**7** and **11**, respectively) were less toxic than their parent compounds, whereas their sulfated metabolites (**8** and **12**, respectively) were, at least, as toxic as their counterparts.

Next, we checked the neuroprotective effect of RES, PTER and their metabolites by inducing oxidative stress to SH-SY5Y neuronal cells through H_2O_2 addition and measuring cell viability after treatment with the phenolic metabolites. The co-treatment experiments (adding simultaneously H_2O_2 and the corresponding compound) showed that only PIN glucuronate (**11**) seemed to have a moderate neuroprotective effect under these experimental conditions whereas the rest of compounds, including parent compound PTER, didn´t attenuate the H_2O_2-induced cytotoxicity (Figure 2A and 2B, left) compared to the H_2O_2 control.

In the case of the pretreatment experiments (adding the corresponding compounds previously to H_2O_2 addition), we observed mild neuroprotective effects for every compound at 1 and 10 μM (Figure 2A and 2B, right), and at 100 μM only for the three glucuronated derivatives screened (**5**, **7** and **11**). The rest of compounds didn't show neuroprotection at the highest concentration tested, possibly due to their intrinsic toxicity to neuronal cells (see Figure 1).

In fact, González-Sarrias et al. also found no effect for RES and its metabolites under similar conditions of co-treatment experiments on SH-SY5Y neuronal cells, and only a slight effect under the pre-treatment experiments.[26] On the other hand, they found that other phenolic natural products such as gallic acid, ellagic acid, 3,4-dihydroxyphenylpropionic acid and 3,4-dihydroxyphenylacetic acid, at 10 μM concentration, significantly attenuated the H_2O_2-induced cytotoxicity in comparison with H_2O_2 treatment alone.

Effects on Intracellular ROS Accumulation and on REDOX Activity Induced by H_2O_2 Addition. The effects on intracellular ROS levels and REDOX activity in neuronal SH-SY5Y cells upon addition of RES and PTER metabolites are summarized in Figures 3 and 4, respectively. The protective effect of the metabolites on H_2O_2-induced oxidative stress was determined at 2h incubation time since H_2O_2 diminishes cell viability up to 50% at 24h for some compounds (see Figure 2). The intracellular ROS accumulation and REDOX activity in the cells with each metabolite alone (without H_2O_2), was measured 6 h after treatments.

In absence of H_2O_2, the intracellular ROS levels in SH-SY5Y cells was slightly lower than in control cells after treatment with RES and its metabolites (Figure 3a, left). This is particularly true for RES (**1**). In the presence of PTER and its metabolites, ROS levels were very close to the control basal levels (except for compound **8**, see Figure 3b, left).

In the case of metabolite and H_2O_2 co-treatments (Figures 3a and 3b, center), most compounds were able to decrease the ROS levels in comparison with the H_2O_2 control (H_2O_2 triggers ROS production up to a 40%). Some compounds were even capable of diminishing ROS production to

levels below the basal levels before H_2O_2 addition (see compounds **1**, **3** and **8**, Figures 3a and 3b, center). Some PTER metabolites (**7**, **10-12)** were active alleviating ROS production at 10 and 100 μM, but not at 1 μM.

In the case of pre-incubation with RES, PTER or their metabolites before H_2O_2 addition (Figures 3a and 3b, right), again, most of the compounds were able to decrease the ROS levels compared to the H_2O_2 control. Remarkably, all PTER metabolites (except compound **7** at 1 μM) were capable of restoring ROS production under the basal levels before H_2O_2 addition. This is also true for RES (**1**) at 10 and 100 μM, but not at 1 μM.

Regarding REDOX activity, RES, PTER and all their metabolites, except **6** and **8** at 100 μM (concentration at which both compounds proved to be very toxic to SH-SY5Y cells, see Figure 1), exhibited an enhanced basal REDOX activity compared to control cells (Figures 4a and 4b, left). The same trend is observed both, in the co-treatment and the pre-treatment experiments with H_2O_2, being most derivatives able to activate the intracellular REDOX activity above the initial levels before H_2O_2 addition (H_2O_2 treatment led to a decrease of REDOX activity of up to a 30%, see Figure 4b, center).

Anti-inflammatory effects of RES, PTER and their Metabolites on LPS-challenged RAW 264.7 macrophages.

All RES, PTER and PIN derivatives except PIN-GlcA (**11**) and PIN-SO_3^- (**12**) showed moderate toxicity for macrophages when incubated for 24 h at concentrations from 100 to 1 μM (Figure 5). Toxicity of RES and its metabolites to RAW macrophages has previously been reported in the literature.[50-51]

Next, we checked the anti-inflammatory capacity of RES, PTER and their metabolites. To do so, we measured cell viability on RAW macrophages after lipopolysacharide (LPS) challenge and after treatment with the different compounds. In general, the co-treatment experiments showed that compounds didn´t alleviate the LPS-induced cytotoxicity (Figure 6A and 6B, left) compared

426 with the LPS control. Only PIN glucuronate (**11**), PIN sulfate (**12**) and RES glucuronate (**5**) at
427 100 μM had a moderate protective effect under these experimental conditions. This result can be
428 clearly explained by the intrinsic toxicity of RES, PTER and their metabolites to macrophages.
429 Thus, the only non-cytotoxic compounds were the ones exerting some anti-inflammatory effect
430 (see Figures 5, 6A and 6B, left).

431 Surprisingly, the pretreatment experiments showed mild anti-inflammatory activity for almost all
432 compounds at 1 and 10 μM concentration (Figure 6A and 6B, right), and also at 100 μM for the
433 three glucuronated metabolites screened (**5**, **7** and **11**). The rest of the compounds didn´t show
434 anti-inflammatory activity at the highest concentration tested due to their toxicity to RAW
435 macrophages (see Figure 5).

436 Finally, the inhibition of IL-6 and NO inflammatory markers on RAW macrophages were
437 assayed for the metabolites showing the best results on the previous experiments (compounds **5**,
438 **7** and **11**). RES and PTER were included as controls and LPS was used as inflammatory trigger.

439 Only PIN glucuronate (**11**) showed a promising inhibitory activity, both on IL-6 (ca. 20%
440 inhibition) and NO (ca. 85% inhibition) values (see Figure 7). PTER showed a moderate NO
441 inhibition (ca. 20%) and very mild IL-6 amelioration. RES glucuronate (**5**) exhibited a mild IL-6
442 inhibition (ca. 5-10%), whereas no inhibition was observed in the production of NO. Both RES
443 and PTER glucuronate (**1** and **7**, respectively) showed no inhibition under these experimental
444 conditions. TNF-α was also measured but no inhibition was observed for PTER or RES
445 metabolites.

446 RES and PTER have been reported in the literature to inhibit both IL-6 and NO to certain
447 extent.[50,52] In any case, it has been described that RES is toxic to RAW macrophages and that
448 stimulation with LPS reduces its toxicity via a mechanism that involves activation of toll like
449 receptor 4.[53] In our case, the lack of activity could be explained based on the high observed
450 toxicity of our metabolites at the concentration used in the ELISA experiments (see Figure 5).
451 Other explanations could be the lower activation produced by LPS in this set of experiments

compared to previous assays carried out in our laboratory (data not shown), which could be due to differences in cells conditions (passage number, cell cycle, etc).

In summary, 3-methyl-4´-glucuronate-resveratrol (**11**) prevented neuronal death via attenuation of ROS levels and increased REDOX activity in SH-SY5Y cells. This metabolite was also able to ameliorate LPS-mediated inflammation on macrophages via inhibition of IL-6 and NO production. Thus, RES and PTER metabolites could be playing and active role on the neuroprotective and anti-inflammatory activities reported for this family of compounds.

Abbreviations used

H2DCFDA , 2′,7′-dichlorodihydrofluorescein diacetate; DMSO, dimethyl sulfoxide; DMEM, Dubelco minimal essential medium; FBS, fetal bovine serum; MTT, 3-(4,5-dimethyl-2-thiazolyl)-2,5-diphenyl-2H-tetrazolium bromide; PBS, phosphate-buffered saline; ROS, reactive oxygen species; REDOX, reduction-oxidation activity; RES, trans-resveratrol; PTER, Pterostilbene; PIN, Pinostilbene; SD, standard deviation; sulf, sulfate; LPS, lipopolysacharide; *IL-6,* interleukin 6; NO, nitric oxide; H_2O, water; H_2O_2, oxygen peroxide solution; MeOH, methanol; CH_2Cl_2; methylene chloride; THF, tetrahydrofurane ;NEt_3, triethylamine; CD_3OD, deuterated methanol; $CDCl_3$, deuterated chloroform; D_2O, deuterated water; HRMS, high resolution mass spectrometry; ES, electrospray; Calcd., calculated; KF, potassium fluoride; K_2CO_3, potassium carbonate; KOH, potassium hydroxide; RP-C18, reversed-phase high performance liquid chromatography column packet with octadecyl carbon chain (C18)-bonded silica; $BF_3 \cdot OEt_2$, Boron trifluoride diethyl etherate; DMF dimethylformamide, TBDMSCl, tert-butyl di-methyl silyl chloride; EtOAc, ethyl acetate; Na_2SO_4, sodium sulfate anhydrous; MHz, Mega hertz; TLC, thin layer chromatography; ppm, parts per million; 2D, bi-dimimentional; NMR, nuclear magnetic resonance; COSY, correlated spectroscopy; TOCSY, total correlated spectroscopy ; ROESY, rotating-frame overhauser spectroscopy; HMQC, Heteronuclear Multiple-Quantum Correlation; ELISA, Enzyme-linked immunosorbent assays; GlcAc, glucuronic acid; SO_3^-, sulfate.

AUTHOR INFORMATION

Corresponding Authors

*P.P: phone, +34-958181621; E-mail: pablo@ipb.csic.es

*J.C.M: phone, +34-958181644; E-mail: jcmorales@ipb.csic.es

ORCID

Juan Carlos Morales: 0000-0003-2400-405X

Pablo Peñalver: 0000-0002-2884-282X

ACKNOWLEDGEMENTS

This work was supported by the Junta de Andalucía (P11-FQM-7316 and P12-FQM-1553) and FEDER funds from the EU are gratefully acknowledged. PP´s work was supported by Junta de Andalucía (P11-FQM-7316).

Appendix A. Supplementary data

^{1}H and ^{13}C-NMR spectra of the new PTER and PIN derivatives synthesized can be found at:

NOTES

The authors declare no competing financial interest.

REFERENCES

(1) Tabner, B. J.; El-Agnaf, O. M.; Turnbull, S.; German, M. J.; Paleologou, K. E.; Hayashi, Y.; Cooper, L. J.; Fullwood, N. J.; Allsop, D. Hydrogen peroxide is generated during the very early stages of aggregation of the amyloid peptides implicated in Alzheimer disease and familial British dementia. *J. Biol. Chem*. **2005**, *280*, 35789-35792.

(2) Uttara, B.; Singh, A. V.; Zamboni, P.; Mahajan, R. T. Oxidative stress and neurodegenerative diseases: a review of upstream and downstream antioxidant therapeutic options. *Curr. Neuropharmacol*. **2009**, *7*, 65-74.

(3) Rosini, M.; Simoni, E.; Milelli, A.; Minarini, A.; Melchiorre, C. Oxidative stress in Alzheimer's disease: are we connecting the dots? *J. Med. Chem.* **2014**, *57*, 2821-2831.

(4) Medzhitov, R. Origin and physiological roles of inflammation. *Nature.* **2008**, *454* (7203), 428-435.

(5) Lawrence, T. The nuclear factor NF-kappa B pathway in inflammation, Cold Spring Harb. *Perspect. Biol.* **2009**, *1* (6), a001651.

(6) Lin, W.W.; Karin, M. A. cytokine-mediated link between innate immunity, inflammation, and cancer. *J. Clin. Invest.* **2007**, *117* (5), 1175-1183.

(7) Karin, M.; Ben-Neriah, Y. Phosphorylation meets ubiquitination: the control of NF-κB activity. *Annu. Rev. Immunol.* **2000**, *18* (1), 621-663.

(8) Müller, J.M.; Ziegler-Heitbrock, H.W.; Baeuerle, P.A. Nuclear factor kappa B, a mediator of lipopolysaccharide effects. *Immunobiology* 1993, *187* (3-5), 233-256.

(9) Singh, M.; Arseneault, M.; Sanderson, T.; Murthy, V.; Ramassamy, C. Challenges for research on polyphenols from foods in Alzheimer's disease: bioavailability, metabolism, and cellular and molecular mechanisms. *J. Agric. Food Chem*. **2008**, *56*, 4855-4873.

(10) Panickar, K. S.; Jang, S. Dietary and plant polyphenols exert neuroprotective effects and improve cognitive function in cerebral ischemia. *Recent Pat. Food, Nutr. Agric.* **2013**, *5*, 128-143.

(11) Ahmed, A. H.; Subaiea, G. M.; Eid, A.; Li, L.; Seeram, N. P.; Zawia, N. H. Pomegranate extract modulates processing of amyloid-β precursor protein in an aged Alzheimer's disease animal model. *Curr. Alzheimer Res.* **2014**, *11*, 834-843.

(12) Hartman, R. E.; Shah, A.; Fagan, A. M.; Schwetye, K. E.; Parsadanian, M.; Schulman, R. N.; Finn, M. B.; Holtzman, D. M. Pomegranate juice decreases amyloid load and improves behavior in a mouse model of Alzheimer's disease. *Neurobiol. Dis.* **2006**, *24*, 506-515.

(13) Rojanathammanee, L.; Puig, K. L.; Combs, C. K. Pomegranate polyphenols and extract inhibit nuclear factor of activated T-cell activity and microglial activation in vitro and in a transgenic mouse model of Alzheimer disease. *J. Nutr.* **2013**, *143*, 597-605.

(14) Singh, N.; Agrawal, M.; Doré, S. Neuroprotective properties and mechanisms of resveratrol in in vitro and in vivo experimental cerebral stroke models. *ACS Chem. Neurosci.* **2013**, *4*, 1151-1162.

(15) Baojian, W.; Sumit, B.; Shengnan, M.; Xiaoqiang, W.; Ming, H. Regioselective Sulfation and Glucuronidation of Phenolics: Insights into the Structural Basis. *Curr Drug Metab.* **2011**, *12*(9), 900-916.

(16) Selma, M. V.; Espín, J. C.; Tomás-Barberán, F. A. Interaction between phenolics and gut microbiota: role in human health. *J. Agric. Food Chem.* **2009**, *57*, 6485-6501.

(17) Ferruzzi, M. G.; Lobo, J. K.; Janle, E. M.; Cooper, B.; Simon, J. E.; Wu, Q. L.; Welch, C.; Ho, L.; Weaver, C.; Pasinetti, G. M. Bioavailability of gallic acid and catechins from grape seed polyphenol extract is improved by repeated dosing in rats: implications for treatment in Alzheimer's disease. *J. Alzheimer Dis.* **2009**, *18*, 113-124.

(18) Gasperotti, M.; Passamonti, S.; Tramer, F.; Masuero, D.; Guella, G.; Mattivi, F.; Vrhovsek, U. Fate of microbial metabolites of dietary polyphenols in rats: is the brain their target destination? *ACS Chem. Neurosci.* **2015**, *6*, 1341-1352.

(19) Yan, L.; Yin, P.; Ma, C.; Liu, Y. Method development and validation for pharmacokinetic and tissue distributions of ellagic acid using ultrahigh performance liquid chromatography-tandem mass spectrometry (UPLC-MS/MS). *Molecules.* **2014**, *19*, 18923-18935.

(20) Azorín-Ortuño, M.; Yáñez-Gascón, M. J.; Vallejo, F.; Pallarés, F. J.; Larrosa, M.; Lucas, R.; Morales, J. C.; Tomás-Barberán, F. A.; García-Conesa, M. T.; Espín, J. C. Metabolites and tissue distribution of resveratrol in the pig. *Mol. Nutr. Food Res.* **2011**, *55*, 1154-1168.

(21) Andres-Lacueva, C.; Shukitt-Hale, B.; Galli, R. L.; Jauregui, O.; Lamuela-Raventos, R. M.; Joseph, J. A. Anthocyanins in aged blueberry-fed rats are found centrally and may enhance memory. *Nutr. Neurosci.* **2005**, *8*, 111-120.

(22) Fornasaro, S.; Ziberna, L.; Gasperotti, M.; Tramer, F.; Vrhovšek, U.; Mattivi, F.; Passamonti, S. Determination of cyanidin-3-glucoside in rat brain, liver and kidneys by UPLC/MS-MS and its application to a short-term phamacokinetic study. *Sci. Rep.* **2016**, *6*, 22815.

(23) Del Rio, D.; Rodriguez-Mateos, A.; Spencer, J. P.; Tognolini, M.; Borges, G.; Crozier, A. Dietary (poly)phenolics in human health: structures, bioavailability, and evidence of protective effects against chronic diseases. *Antioxid. Redox Signaling* **2013**, *18*, 1818-1892.

(24) Hu, N.; Yu, J.T.; Tan, L.; Wang, Y.L.; Sun, L.; Tan, L. Nutrition and the risk of Alzheimer's diseases. *BioMed Res. Int.* **2013**, *2013*, 524820.

(25) Hornedo-Ortega, R.; Álvarez-Fernández, M.A.; Cerezo, A.B.; Richard, T.; Troncoso, A.M.; Garcia-Parrilla, M.C. Protocatechuic Acid: Inhibition of Fibril Formation, Destabilization of Preformed Fibrils of Amyloid-β and α-Synuclein, and Neuroprotection. *J. Agric. Food Chem.* **2016**, *64* (41), 7722-7732.

(26) González-Sarrías, A.; Núñez-Sánchez, M.A.; Tomás-Barberán, F.A.; Espín, J.C. Neuroprotective Effects of Bioavailable Polyphenol-Derived Metabolites against Oxidative Stress-Induced Cytotoxicity in Human Neuroblastoma SH-SY5Y Cells. *J. Agric. Food Chem.* **2017**, *65*, 752-758.

(27) Kapetanovic, I.M.; Muzzio, M.; Huang, Z.; Thompson, T.N.; McCormick, D.L. Pharmacokinetics, oral bioavailability, and metabolic profile of resveratrol and its dimethylether analog, pterostilbene, in rats. *Cancer Chemother. Pharmacol.* **2011**, *68* (3), 593-601.

(28) Nikhil, K; Sharan, S.; Palla, S.R.; Sondhi, S.M.; Peddinti, R.K.; Roy, P. Understanding the mode of action of a pterostilbene derivative as anti-inflammatory agent. *Int. Immunopharm.* **2015**, *28*, 10-21.

579 (29) Remsberg, C.M.; Yáñez, J.A.; Ohgami, Y.; Vega-Villa, K.R.; Rimando, A.M.; Davies, N.M.
580 Pharmacometrics of pterostilbene: preclinical pharmacokinetics and metabolism, anticancer,
581 antiinflammatory, antioxidant and analgesic activity. *Phytother. Res.* **2008**, *22* (2), 169-179.

582 (30) Pan, M.H.; Chang, Y.H.; Tsai, M.L.; Lai, C.S.; Ho, S.Y.; Badmaev, V.; Ho, C.T.
583 Pterostilbene suppressed lipopolysaccharide-induced up-expression of iNOS and COX-2 in
584 murine macrophages. *J. Agric. Food Chem.* **2008**, *56* (16), 7502-7509.

585 (31) Chakraborty, A.; Gupta, N.; Ghosh, K.; Roy, P. In vitro evaluation of the cytotoxic,
586 antiproliferative and anti-oxidant properties of pterostilbene isolated from Pterocarpus
587 marsupium. *Toxicol. In Vitro.* **2010**, *24,* 1215-1228.

588 (32) Chakraborty, A.; Bodipati, N.; Demonacos, M.K.; Peddinti, R.; Ghosh, K.; Roy, P. Long
589 term induction by pterostilbene results in autophagy and cellular differentiation in MCF-7 cells
590 via ROS dependent pathway. *Mol. Cell. Endocrinol.* **2012**, *355,* 25-40.

591 (33) McCormack, D.; McFadden, D. A Review of Pterostilbene Antioxidant Activity and Disease
592 Modification. *Oxid. Med. Cell. Longev.* **2013**, Article ID 575482, 15 pages.

593 (34) Shao, X.; Chen, X.; Badmaev, V.; Ho, C-T.; Sang, S.; Structural identification of mouse
594 urinary metabolites of pterostilbene using liquid chromatography/tandem mass spectrometry.
595 *Rapid Commun. Mass Spectrom.* **2010**, *24*, 1770–1778.

596 (35) Boralle, N.; Gottlieb, H.E.; Gottlieb, O.R.; Kubitzki, K.; Lopes, L.M.X.; Yoshida, M.;
597 Young, M.C.M. Oligostilbenoids from Gnetum venosum. *Phytochem.* **1993**, *34* (5), 1403-1407.

598 (36) Tyukavkina, N. A.; Gromova, A. S.; Lutskii, V. I.; Voronov, V. K. Hydroxystilbenes from
599 the bark of Pinus sibirica. *Chem. Nat. Compd*. **1972**, *8* (5), 570-572.

600 (37).; Wu, X.; Cai, X.; Song, M.; Zheng, J.; Pan, C.; Qiu, P.; Zhang, L.; Zhou, S.; Tang, Z.; Xiao,
601 H. Identification of pinostilbene as a major colonic metabolite of pterostilbene and its inhibitory
602 effects on colon cancer cells. *Mol Nutr Food Res.* **2016**, *60*(9), 1924-32.

(38) Dvorakova, M.; Landa, P. Anti-inflammatory activity of natural stilbenoids: A review. *Pharmacol. Res.* **2017**, *124*, 126-145.

(39) Harding, J.R.; King, C.D.; Perrie, J.A.; Sinnott, D.; Stachulski, A.V. Glucuronidation of steroidal alcohols using iodosugar and imidate donors. *Org Biomol Chem* **2005**, *3*, 1501-1507.

(40) Falomir, E.; Lucas, R.; Penalver, P.; Marti-Centelles, R.; Dupont, A.; Zafra-Gomez, A.; Carda, M.; Morales, J.C. Cytotoxic, antiangiogenic and antitelomerase activity of glucosyl- and acyl- resveratrol prodrugs and resveratrol sulfate metabolites. *Chembiochem* **2016**, *17*, 1343-1348.

(41) Raghuraman, A.; Riaz, M.; Hindle, M.; Desai, U.R. Rapid and efficient microwave-assisted synthesis of highly sulfated organic scaffolds. *Tetrahedron Lett.* **2007**, *48*, 6754-6758.

(42) Al-Horani, R.A.; Desai, U.R. Chemical sulfation of small molecules-advances and challenges. *Tetrahedron* **2010**, *66*, 2907-2918.

(43) Gonzalez-Rey, E.; Anderson, P.; Gonzalez, M.A.; Rico, L.; Buscher, D.; Delgado, M. Human adult stem cells derived from adipose tissue protect against experimental colitis and sepsis. *Gut* **2009**, *58*, 929-939.

(44) Sanchez, S.; Barger, T.; Zhou, L.; Hale, M.; Mytych, D.; Gupta, S.; Swanson, S.J.; Civoli, F. Strategy to confirm the presence of anti-erythropoietin neutralizing antibodies in human serum. *J Pharm Biomed Anal* **2011**, *55*, 1265-1274.

(45) Green, L.C.; Wagner, D.A.; Glogowski, J.S.; Skipper, P.L.; Wishnok, J.S.; Tannenbaum, S.R. Analysis of nitrate, nitrite and [15-N]nitrite in biological fluids. *Ann. Biochem.* **1982**, *126*(1), 131-138.

(46) Puksasook, T.; Kimura, S.; Tadtong, S.; Jiaranaikulwanitch, J.; Pratuangdejkul, J.; Kitphati, W.; Suwanborirux, K.; Saito, N.; Nukoolkarn, V. Semisynthesis and biological evaluation of prenylated resveratrol derivatives as multi-targeted agents for Alzheimer's disease. *J. Nat. Med.* **2017**, *71* (4), 665-682.

(47) Orsini, F.; Verotta, L.; Lecch,i M.; Restano, R.; Curia, G.; Redaelli, E.; Wanke, E. Resveratrol derivatives and their role as potassium channels modulators. *J. Nat. Prod.* **2004**, *67*, 421-426.

(48) Hoshino, J.; Park, E.J.; Kondratyuk, T.P.; Marler, L.; Pezzuto, J.M.; van Breemen, R.B.; Mo, S.; Li, Y.; Cushman, M. Selective synthesis and biological evaluation of sulfate-conjugated resveratrol metabolites. *J. Med. Chem.* **2010**, *53*, 5033-5043.

(49) Lucas, R.; Alcantara, D.; Morales, J. C.; A concise synthesis of glucuronide metabolites of urolithin-B, resveratrol and hydroxytyrosol. *Carbohydr. Res.* **2009**, *344*, 1340-1346.

(50) Peñalver, P.; Belmonte-Reche, E.; Adán, N.; Caro, M.; Mateos-Martín, M.L.; Delgado, M.; González-Rey, E.; Morales, J.C.; Alkylated resveratrol prodrugs and metabolites as potential therapeutics for neurodegenerative diseases. *Eur. J. Med. Chem.* **2018**, *146*, 123-138.

(51) Billack, B.; Radkar, V.; Adiabouah, C. In vitro evaluation of the cytotoxic and anti-proliferative properties of resveratrol and several of its analogs. *Cell Mol Biol Lett.* **2008**, *13*(4),553-69.

(52) Yao, Y.; Liu, K.; Zhao, Y.; Hu, X.; Wang, M. Pterostilbene and 4′-Methoxyresveratrol Inhibited Lipopolysaccharide-Induced Inflammatory Response in RAW264.7 Macrophages. *Molecules* **2018**, *23*(5), 1148.

(53) Achy-Brou, C.A.A.; Billack, B. Lipopolysaccharide Attenuates the Cytotoxicity of Resveratrol in Transformed Mouse Macrophages. *Plant Foods Hum. Nutr.* **2016**, *71*(3), 272-276.

652 **Graphic for table of contents**

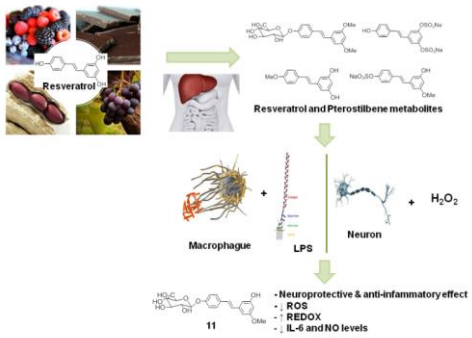

653

654

655 **Table 1.** Resveratrol and pterostilbene derivatives examined in this work.

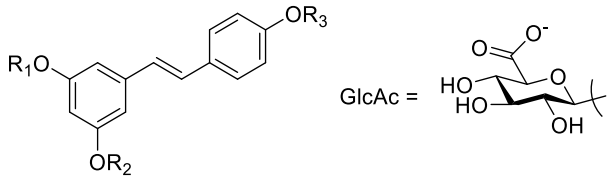

Compound	R_1	R_2	R_3	Compound	R_1	R_2	R_3
RES derivatives				*PTER derivatives*			
RES (1)	H	H	H	**PTER (6)**	Me	Me	H
RES-3-S (2)	SO_3^-	H	H	**PTER-GlcAc (7)**	Me	Me	GlcAc
RES-4'-S (3)	H	H	SO_3^-	**PTER-S (8)**	Me	Me	SO_3^-
RES-3,4'-diS (4)	SO_3^-	H	SO_3^-	**PIN (9)**	Me	H	H
RES-3-GlcAc (5)	GlcAc	H	H	**4'-Me-RES (10)**	H	H	Me
				PIN-4'-GlcAc (11)	Me	H	GlcAc
				PIN-4'-S (12)	Me	H	SO_3^-

656

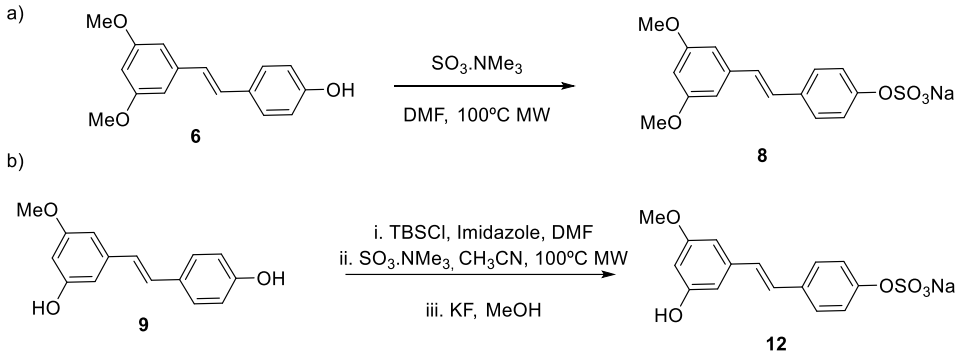

657

658 **Scheme 1**: Synthesis of PTER sulfate metabolite **8** (a) and PIN sulfate metabolite **12** (b)

659

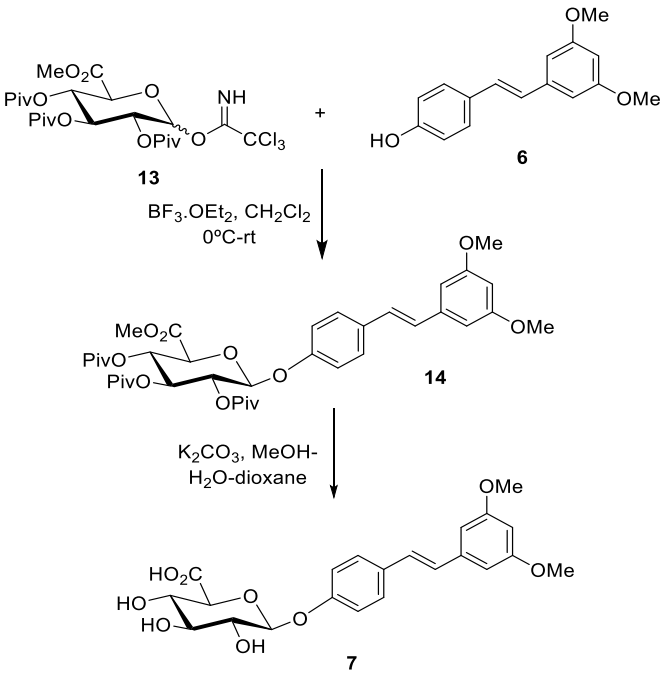

660

661 **Scheme 2**: Synthesis of PTER glucuronic metabolite **7**

662

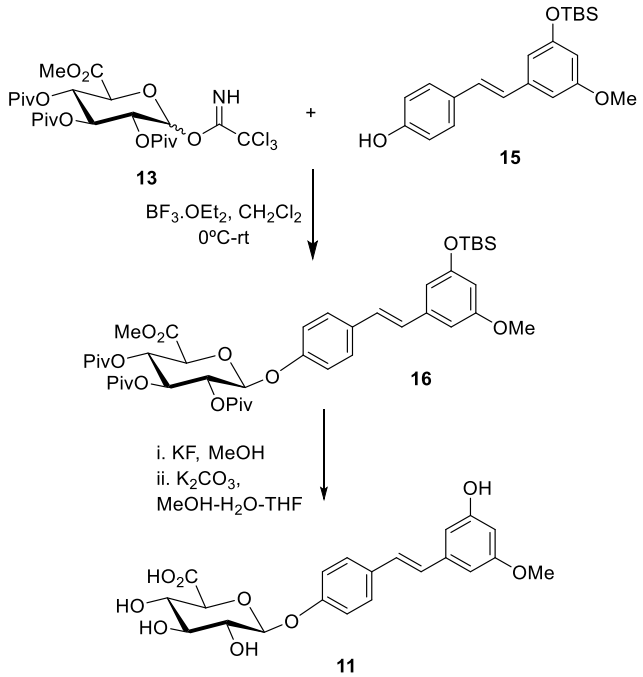

663

664 **Scheme 3:** Synthesis of Pinostilbene glucuronate metabolite **11**

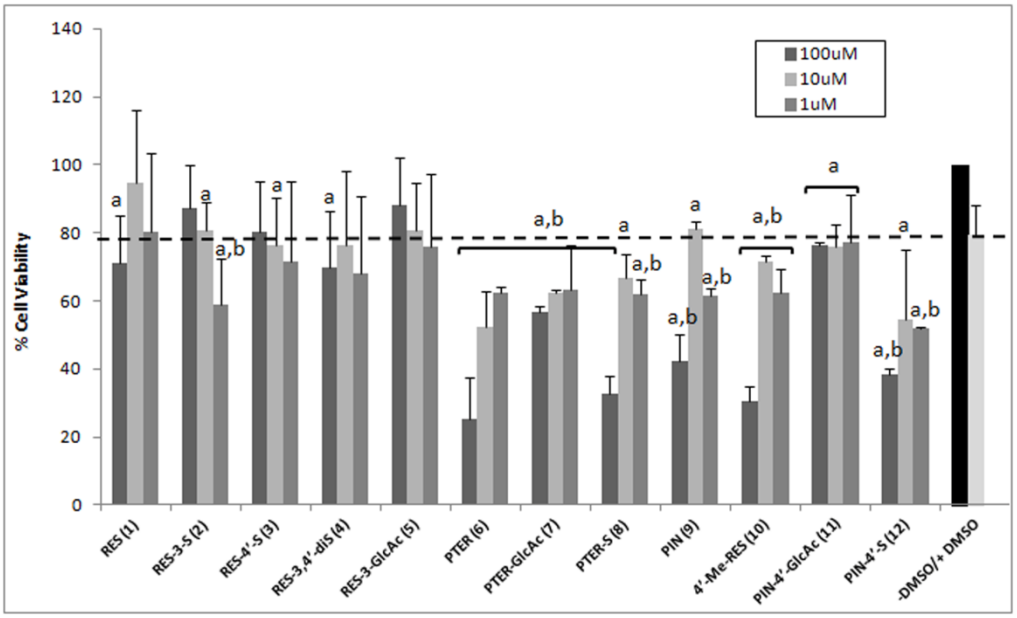

Figure 1. Cytotoxicity of RES and PTER metabolites (100, 10 and 1 μM) in SH-SY5Y neuronal cells. Values (%) are expressed as the mean ± SD (n = 2-4, in quatriplicate). Symbols: **a**, means significant difference ($p < 0.05$) compared to control cells (- DMSO); **b**, means significant difference ($p < 0.05$) compared to DMSO treatment alone.

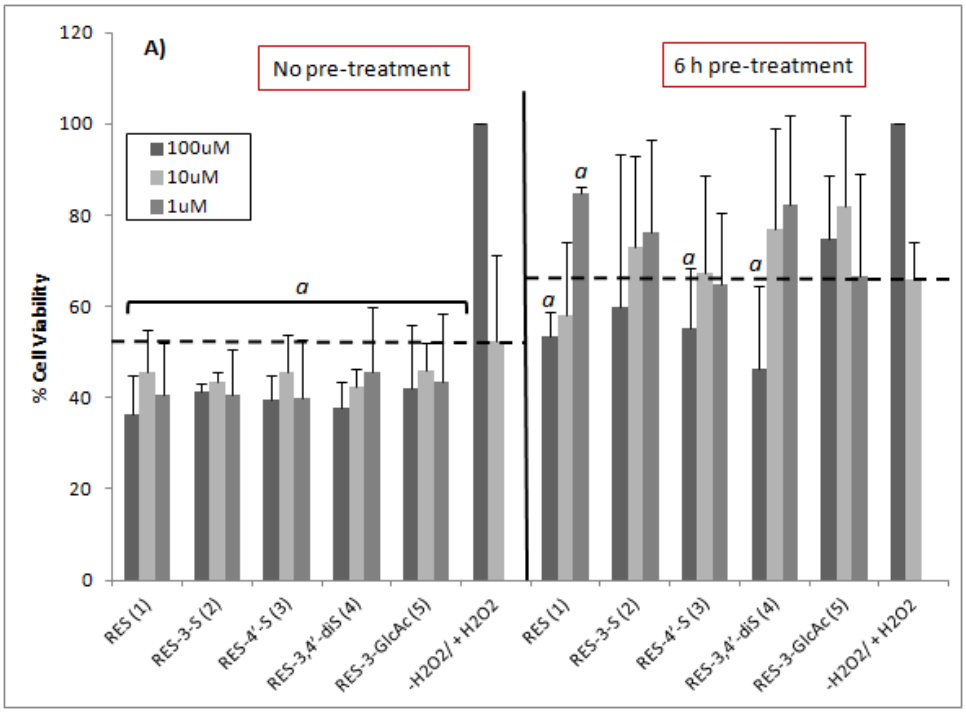

671

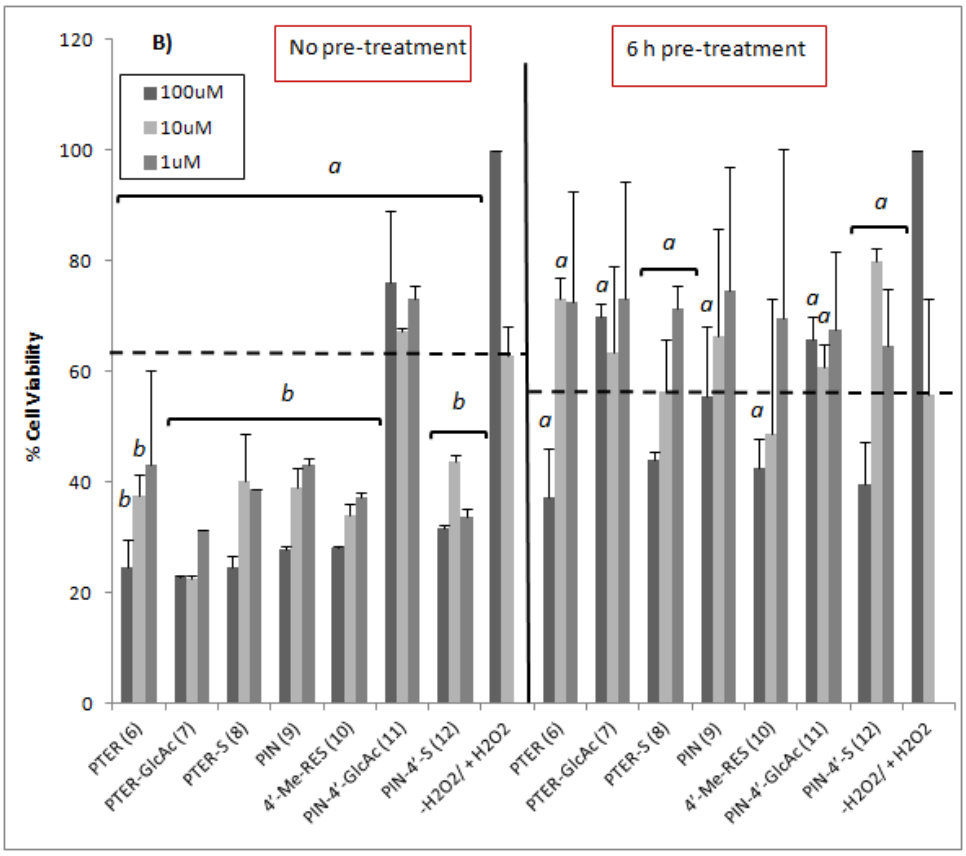

672

673 **Figure 2.** Effect of RES and PTER metabolites (100, 10 and 1 μM) (6 h pretreatment, 24 h cotreatment
674 with H_2O_2, 100 μM) in SH-SY5Y neuronal cells; A) RES metabolites; B) PTER metabolites. Values (%)
675 are expressed as the mean ± SD (n = 2-4, in quatriplicate). Symbols: **a**, means significant difference ($p <$

0.05) compared to control cells; **b**, means significant difference ($p < 0.05$) compared to H_2O_2 treatment alone.

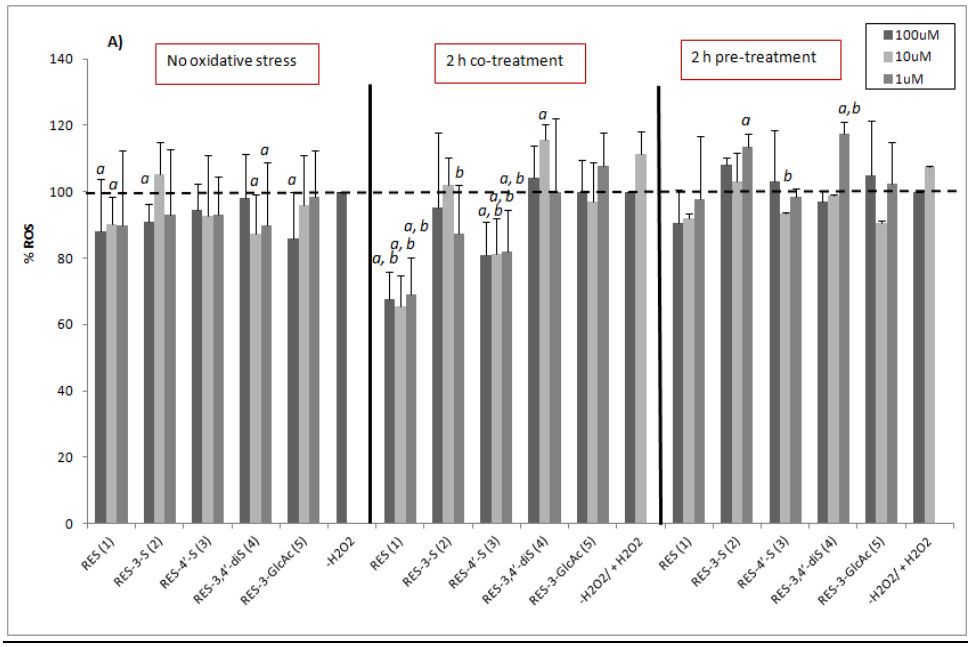

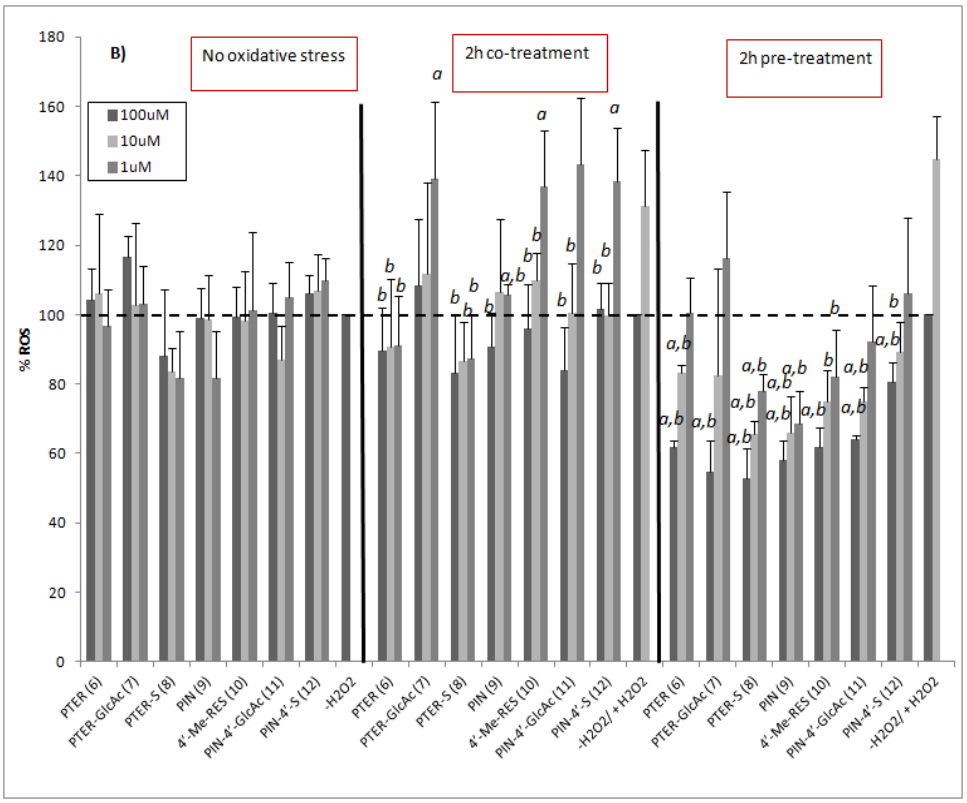

Figure 3. Effect of RES and PTER metabolites (100, 10 and 1 μM) on ROS generation in SH-SY5Y neuronal cells; A) RES metabolites; B) PTER metabolites. Values (%) are expressed as the mean ± SD (n

682 = 2-4, in quatriplicate). Symbols: **a**, means significant difference ($p < 0.05$) compared to control cells; **b**,

683 means significant difference ($p < 0.05$) compared to H_2O_2 treatment alone.

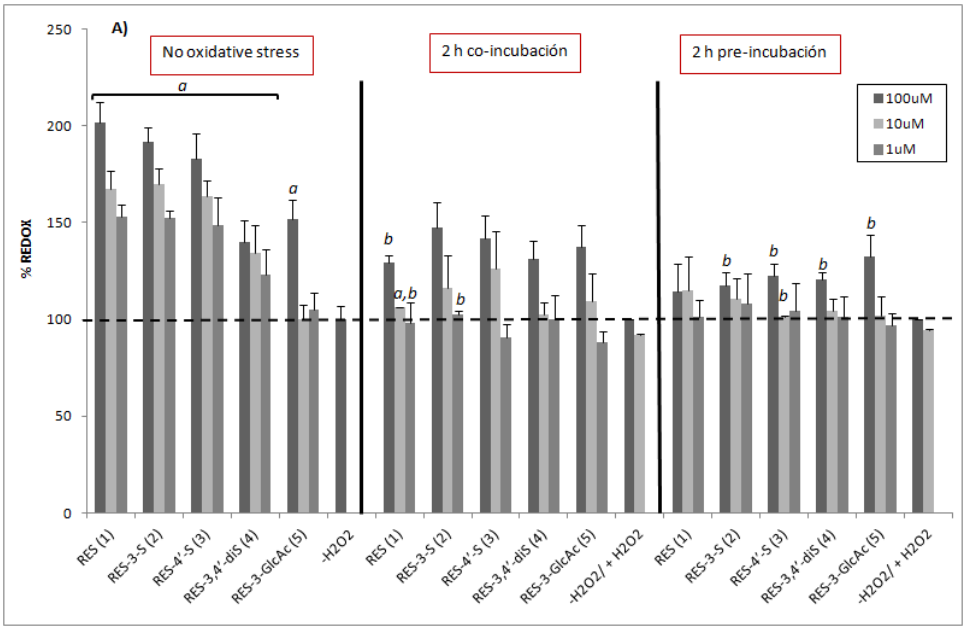

684

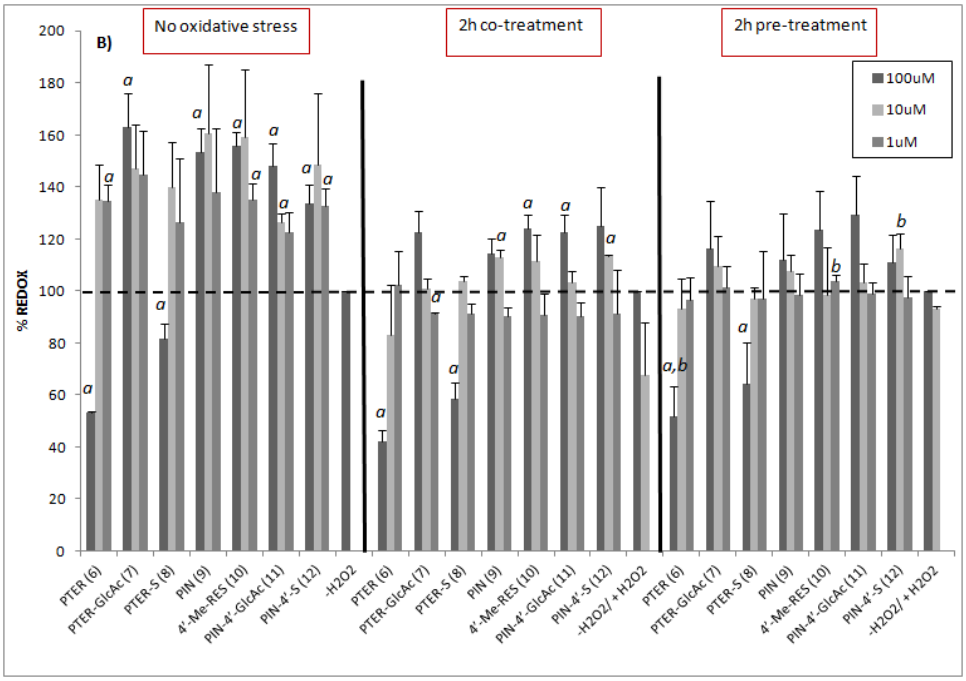

685

686 **Figure 4.** Effect of RES and PTER metabolites (100, 10 and 1 µM) on REDOX activity in SH-SY5Y

687 neuronal cells; A) RES metabolites; B) PTER metabolites. Values (%) are expressed as the mean ± SD (n

688 = 2-4, in quatriplicate). Symbols: **a**, means significant difference ($p < 0.05$) compared to control cells; **b**,

689 means significant difference ($p < 0.05$) compared to H_2O_2 treatment alone.

690 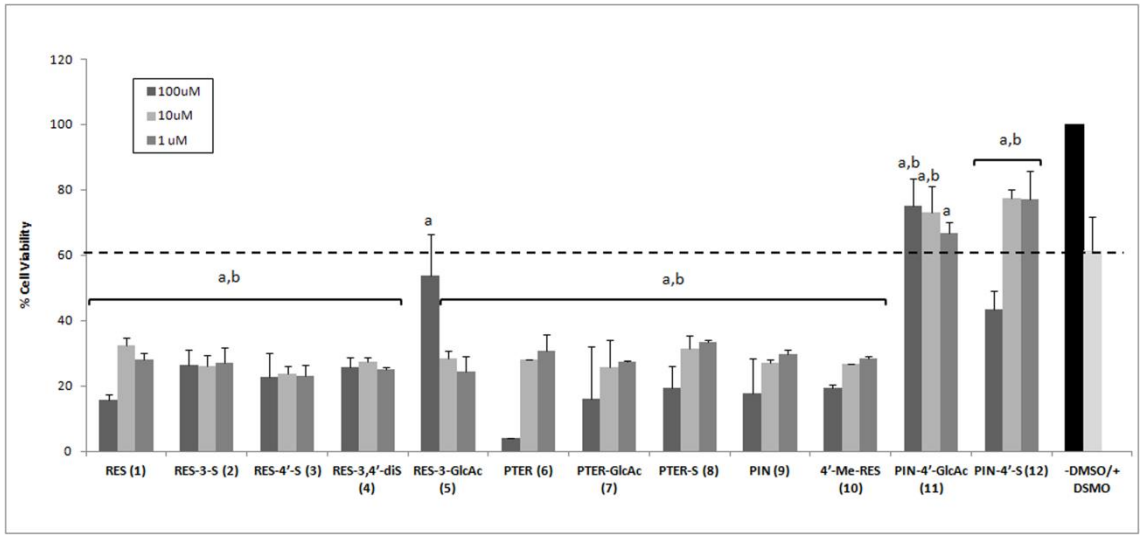

691 **Figure 5.** Toxicity of RES and PTER metabolites (100, 10 and 1 μM) (24 h co-treatment with LPS) in
692 RAW 264.7 macrophages. Values (%) are expressed as the mean ± SD (n = 2-4, in quatriplicate). Symbols:
693 **a**, means significant difference ($p < 0.05$) compared to control cells (- DMSO); **b**, means significant
694 difference ($p < 0.05$) compared to DMSO treatment alone.

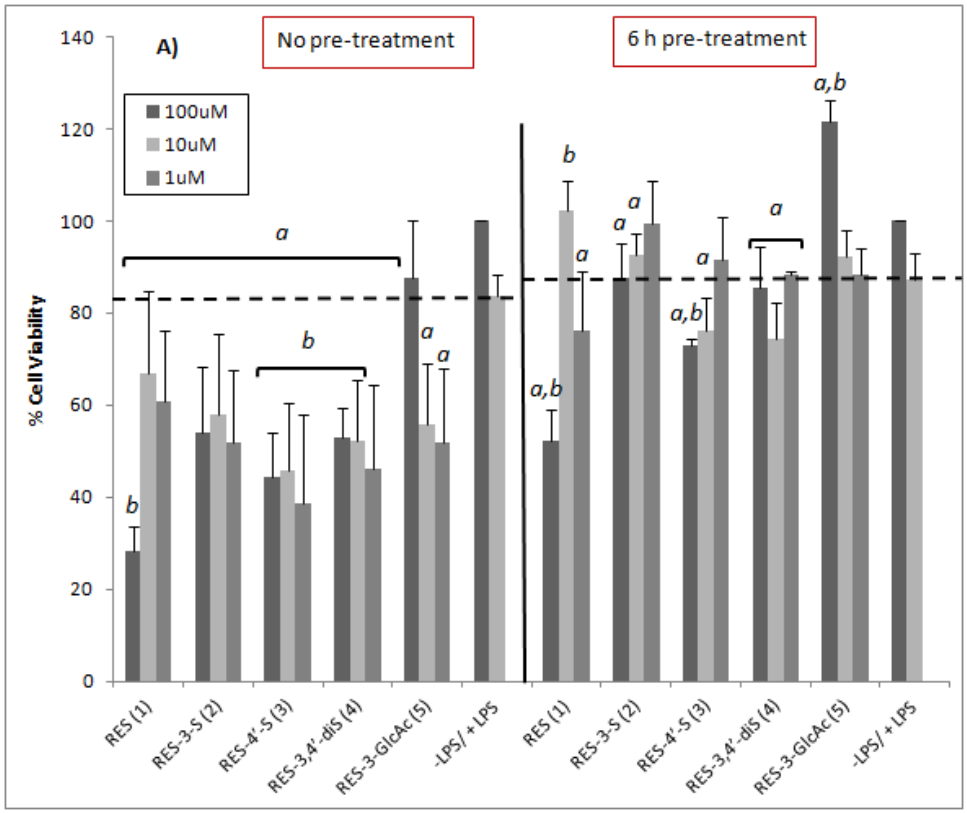

695

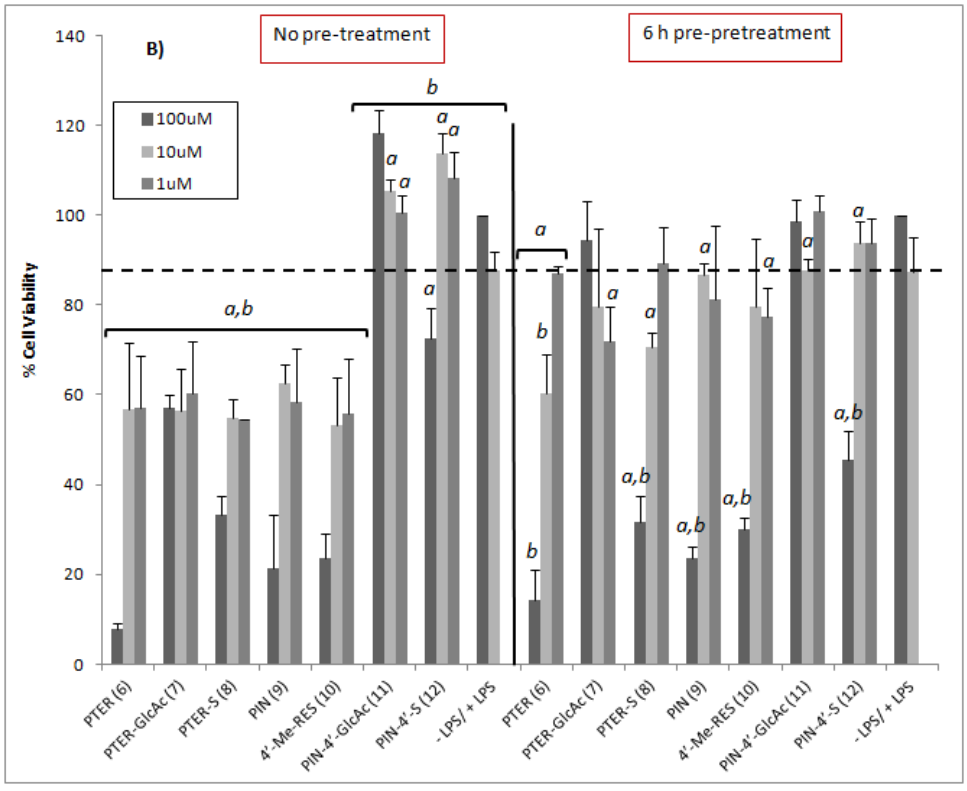

696

697 **Figure 6.** Effect of RES and PTER metabolites (100, 10 and 1 μM) (6 h pretreatment, 24 h cotreatment
698 with LPS) in RAW 264.7 macrophages; A) RES metabolites; B) PTER metabolites. Values (%) are

699 expressed as the mean ± SD (n = 2-4, in quatriplicate). Symbols: **a**, means significant difference ($p < 0.05$)
700 compared to control cells; **b**, means significant difference ($p < 0.05$) compared to H_2O_2 treatment alone.

701

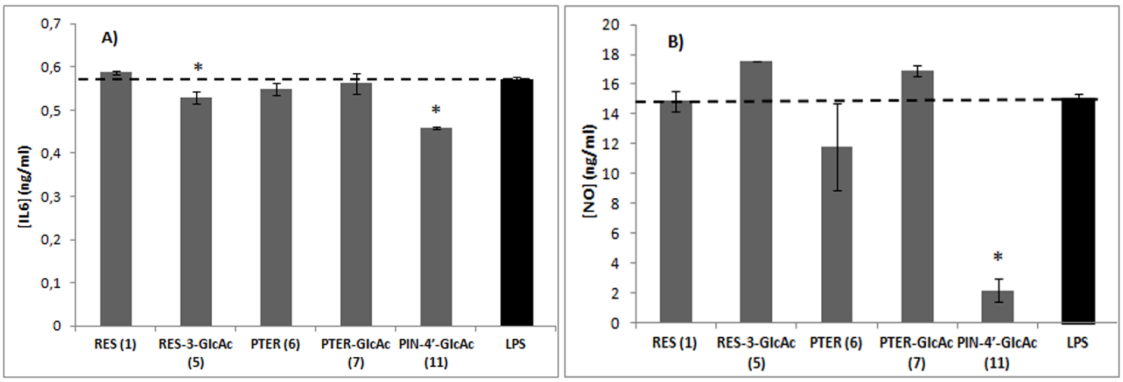

702

703 **Figure 7.** Effect of RES, PTER and their more promising metabolites on the pro-inflamatory makers
704 inhibition (10 μM, 24 h cotreatment with LPS) in RAW 264.7 macrophages; A) IL-6; B) NO Values (%)
705 are expressed as the mean ± SD. Symbols: (*) means significant difference ($p < 0.05$) compared to LPS
706 treatment alone.

707